Motion Control of a 4-DOF Cable-Driven Upper Limb Exoskeleton

Jianhua Wang[1], Wang Li[1], Weihai Chen[1], Jianbin Zhang[2,*]

***Abstract*—This paper presents the motion control of a 4-DOF cable-driven upper limb exoskeleton. The exoskeleton consists of a 3-DOF shoulder module and a 1-DOF elbow module, with six cables are routed through the exoskeleton cuffs to drive the whole upper limb motion, each module can be controlled independently. This design preserves the advantages with cable-driven parallel mechanisms, and introduces the advantages in having a serial kinematic structure. To control the motion of the exoskeleton along desired trajectories in space, nonlinear feedforward control laws in the cable length coordinates are used. Taking account of the effect of redundancy on actuation, optimal tension distribution is considered in the control laws. Trajectories tracking capability was demonstrated through experiments with the prototype of exoskeleton.**

***Index Terms*—cable-driven, exoskeleton, motion control, tension distribution**

I. INTRODUCTION

Stroke can cause permanent damage to the brain's nervous system, thereby impairing the nerve pathways that the brain innervates the limbs [1]. Stroke has become the second most common cause of death and disability in the world [2]. The burden of stroke will increase dramatically in the next 20 years due to the aggravation of population aging [3] [4]. Stroke survivors often suffer from hemiplegia, paraplegia, and other motor impairments, Extremely serious impact on patients themselves and their families. Combining robotics with rehabilitation medicine can make up for the shortcomings of traditional rehabilitation training and gradually become an important branch in the field of medical robotics.

The purpose of the upper limb rehabilitation robot is to help patients carry out rehabilitation training of upper limb movement. It can be divided into two main categories, one is terminal traction type, the other is exoskeleton type [5] [6] [7] [8]. MIT-MANUS is the earliest rehabilitation training robot developed by MIT. MIT-MANUS belongs to the terminal traction type. It uses planar five-bar linkage mechanism to achieve 2-DOF rehabilitation exercise at the end [6] [9]. In 2000, an upper limb rehabilitation robot, ARM-Guide [10], was developed by the University of California, Irvine. The patients fixed their arms on linear guides and moved back and forth along the guideways. At the same time, the slides were made to have two degrees of freedom, pitch and yaw by two motors as a whole. The motion amplitude and intensity of the affected limbs were monitored in real time, and the motion function of the patients was assessed. A 6-DOF MIME(MIRROR-IMAGE MOTION ENABLER) rehabilitation robot has been developed from PUMA560 industrial robot by Stanford University [**?**]. By analyzing the motion trajectory of the patient's healthy upper limb, the robot can drive the affected arm to mirror motion based on the reference trajectory. The ARMin series [11] [12] exoskeleton rehabilitation robots jointly developed by Zurich Federal Institute of Technology have the motion assistance function of seven joints of the human arm. At present, Hocoma has developed the corresponding commercial upper limb rehabilitation robot ArmeorPower [13] based on ARMin.

The traditional rehabilitation exoskeleton robot has many degrees of freedom, which results in heavy body weight and inflexible movement [14]. The CADEN-7 [5] Rehabilitation Exoskeleton Robot developed by Washington University can completely reproduce the seven-degree-of-freedom movement of upper limb glenohumeral joint, elbow joint and wrist joint. There is also the L-Exos [15] five-degree-of-freedom rehabilitation robot jointly developed by the University of Pisa and other units in Italy. Its mechanical structure is similar to CADEN-7, and it is also a single-joint rope transmission design based on pulley line. The REPERT Upper Limb Rehabilitation Exoskeleton Robot [16] studied by Arizona State University uses pneumatic artificial muscle (PMA) as exoskeleton drive to achieve five degrees of freedom movement of upper limbs.

The end-traction rehabilitation robot connects the end of the robot with the end of the upper limb of the patient and drives the movement of the affected limb through the motion of the robot [8] [9]. Generally, the common series link is the main body, but it can not fit with the limb of the patient, and can not complete the precise motion-aided training in the space of the affected limb joints [17]. Because of its simple structure, low production cost, the early upper limb rehabilitation robot is not able to complete the motion-aided training in the space of the Most of them are of this type. Exoskeleton-type upper limb rehabilitation robot is directly worn outside the upper limb, aligning the rotation axis of the manipulator with the joint axis of the human body. Exoskeleton-type rehabilitation robot exerts auxiliary force on the exterior of the limb to realize the movement of joint space and Cartesian space. Compared with the end-driven rehabilitation robot, exoskeleton-type rehabilitation robot is more flexible in motion control and has become Kang at present. A hotspot in the field of complex robots.

In order to reduce the weight of the robot and maintain

[1]Jianhua Wang, Wang Li, Weihai Chen are with School of Automation Science and Electrical Engineering, Beihang University, 100191 Beijing, China (email: jhwangbuaa@126.com, 847205053@qq.com, whchenbuaa@126.com)

[2]Jianbin Zhang is with School of Mechanical Engineering and Automation, Beihang University, 100191 Beijing, China(email: jbzhangbuaa@163.com)

*Corresponding author

the flexibility of the robot, researchers at home and abroad have studied the use of cable-driven or synchronous belt-driven remote transmission technology to separate the driving unit from the exoskeleton, so as to achieve the exoskeleton lightweight design [18]. At the same time, some upper extremity exoskeleton robots add adjustable mechanisms to adapt to the physiological size of upper limbs of different wearers, or add active or passive additional degrees of freedom to achieve joint center alignment [19]. Compared with the traditional motor-driven method, rope-driven method has the advantages of low cost, light weight and easy reconfiguration. It has high adaptability to the wearer. Researchers have extensively studied rope-driven humanoid arm robot [20] [21] [22]. Some scholars have combined rope-driven with rehabilitation robot, and achieved good experimental results.

In this paper, a 4 DOF exoskeleton rehabilitation robot was developed for shoulder and elbow rehabilitation training. To control the motion of the exoskeleton robot along desired trajectories in space, nonlinear feedforward based controller in cable length coordinates are used. The feasibility and effectiveness of this approach is proven in the experiment.

This paper is organized as follows. In section II, we introduce the kinematic model of the upper limb exokeleton, including the prototype of 4 DOF upper limb exoskeleton robot, kinematic and dynamatic model. Control scheme is described in section III. In section IV, experimental results are demonstrated. Finally conclusions are given in Section V.

II. DYNAMIC MODEL OF 4-DOF UPPER LIMB EXOSKELETON

A. Mechanical Structure

Fig.1 shows the mechanical structure of 4-DOF exoskeleton robot, it mainly consist two parts, the shoulder module and the elbow module, which are driven by six cables, the shoulder cuff is fixed to the base frame, all electricial system components are mounted in the base frame, including motors, power, controller. The cable-driven exoskeleton is made up by three cuffs, including shoulder cuff, upper-arm cuff and the forearm cuff. The shoulder cuff is fixed to the base frame, which is static, the upper-arm cuff and forearm cuff are respectively connected with human upper-arm and forearm. To improve the safety and comfort of the exoskeleton on wear's upper extremity, the inner wearable module are made of silicone rubber. Other components of the exoskeleton are made of aluminum or steel.

The exoskeleton is a cable-driven parallel mechanism, which can provide 4-DOF motion for upper limb of wearer. The exoskeleton can be divided into two modules: the 3-DOF shoulder module and the 1-DOF elbow module. The shoulder module consist of shoulder cuff and upper-arm cuff, elbow module consist of upper-arm cuff and fore-arm cuff. Four nylon-coated steel cabes are chosen to actuate 3-DOF of the subject's shoulder joint(abduction/adduction, flexion/extension, inward/outward rotation). These four cables start from shoulder cuff, then through bowden tube and fix on the upper arm cuff. Respectively, the remaining two cables

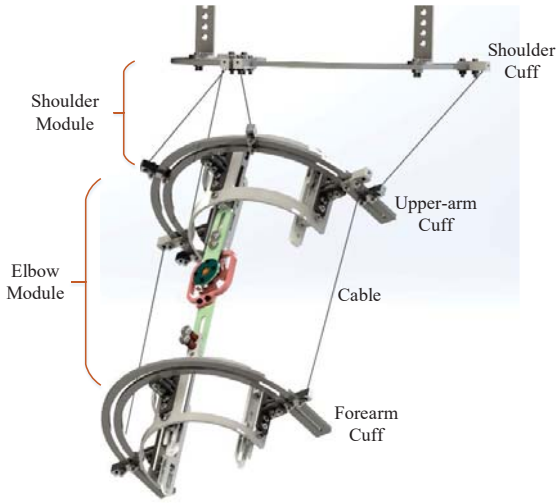

Fig. 1. The 4 DOF upper limb exoskeleton.

start from shouler cuff and end on forearm cuff to acutate 1-DOF of the subject's elbow(flexion/extension). These two cables are started from the base frame and end on upper arm cuff. The cable-driven exoskeleton robot, compared to normal type of exoskeleton, has three advantages:

- prevent the cable collisions between shoulder and elbow module.
- robot is much lighter without motors installed on the joint.
- shoulder module and elbow module can be analyzed separately.

B. Kinematic and Dynamatic Modeling

The forward kinematics of the 4-DOF exoskeleton robot is derived based on the Denavit-Hartenberg(DH) convention. Coordinate i and coordinate $i-1$ were connected by four parameters $a_{i-1}, d_i, \alpha_{i-1}, \theta_i$, these parameters are link length, link twist, link offset and joint angle, respectively. A coordinate frame is attached to each joint to determine DH parameters.

Fig.2 shows the coordinate frame assignment for 4 DOF upper limb exoskeleton, the DH parameters of 4-DOF exoskeleton robot are listed in tablet, the homogeneous transformation matrix ${}^{i}_{0}T$ as a function of the four DH parameters per link $(a_{i-1}, d_i, \alpha_{i-1}, \theta_i)$ defines the transformation between two consecutive frames.

$$ {}^{i-1}_{i}T = Screw(X, a_{i-1}, \alpha_{i-1}) Screw(Z, d_i, \theta_i) \qquad (1) $$

$Screw(Q, r, \phi)$ represents the rotation of angle ϕ and translation of length r around and along the Q axis. The general transformation matrix ${}^{i-1}_{i}T$ for a single link can be obtained as follows:

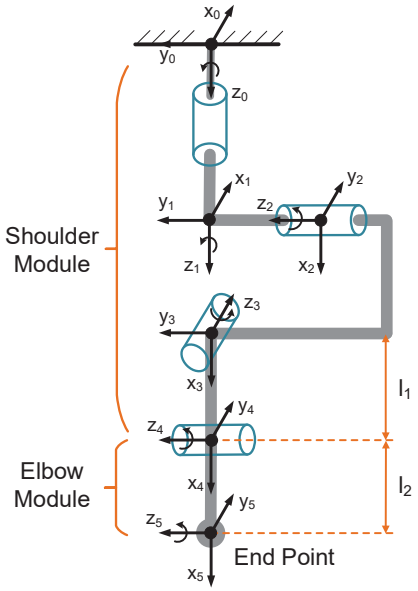

Fig. 2. Schematic diagram of shoulder and elbow module.

$$ {}^{i-1}_{i}T = \begin{bmatrix} c\theta_i & -s\theta_i & 0 & a_{i-1} \\ s\theta_i c\alpha_{i-1} & c\theta_i c\alpha_{i-1} & -s\alpha_{i-1} & -d_i s\alpha_{i-1} \\ s\theta_i s\alpha_{i-1} & c\theta_i s\alpha_{i-1} & c\alpha_{i-1} & d_i c\alpha_{i-1} \\ 0 & 0 & 0 & 1 \end{bmatrix} \quad (2) $$

where $c\theta_i = cos\theta_i$, $s\theta_i = sin\theta_i$, θ_i is the rotation angle of the i-th frame, a_{i-1} is the distance between the axes z_{i-1} and z_i, and is measured along the axis x_{i-1}, d_i is the distance between the axes x_{i-1} and x_i, measured along the axis z_i, α_{i-1} is the rotation angle between x_{i-1} and x_i, measured in a plane normal to z_i.

The DH parameters corresponding to this exoskeleton robot are shown in Table I.

TABLE I
DH PARAMETER FOR 4-DOF EXOSKELETON

i	a_{i-1}	α_{i-1}	d_i	θ_i
1	0	0	0	θ_1
2	0	-π/2	0	θ_2
3	0	π/2	0	θ_3
4	l_1	−π/2	0	θ_4
5	l_2	0	0	0

Homogeneous transformation matrix describing the position and orientation of fram i with respect to frame 0 is defined by ${}^{i}_{0}T$ as:

$$ {}^{i}_{0}T = {}^{1}_{0}T {}^{2}_{1}T \cdots {}^{i}_{i-1}T, \quad i = 1, 2, \cdots 5 \quad (3) $$

Because of the limitation of mechanical structure, such as the intervene between upper limb cuff and shoulder cuff, the feasible rom of exoskeleton is smaller than human arm, the feasible rom of each joint is shown in Table II. The reachable workspace and orientation workspace of upper limb exoskeleton is shown in Fig.3.

TABLE II
ROM OF UPPER EXOSKELETON JOINT

Joint Motion	Range
Shoulder flexion/extension	$[-50°, 50°]$
Shoulder adduction/abduction	$[-45°, 45°]$
Shoulder lateral/medial motion	$[0°, 45°]$
Elbow flexion/extension	$[0°, 70°]$

Then, the feasible workspace of joint space and Cartesian space of exoskeleton is obtained by traversal method. The feasible range of joint angle of exoskeleton is a subset of which of upper limb motion. Before carrying out the assistant training of upper limb exoskeleton, we will check whether the trajectory is in the workspace of exoskeleton.

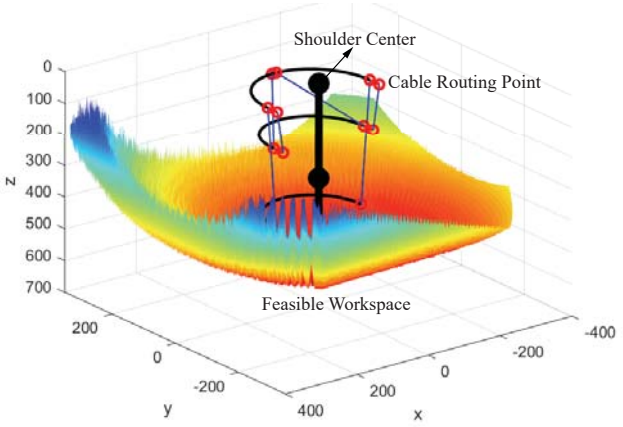

Fig. 3. 4-DOF Exoskeleton feasible workspace.

The dynamic modeling for four degree-of-freedom serial chain robot is derived from Lagrange's equation, which is written as:

$$ M(q)\ddot{q} + C(q, \dot{q}) + G(q) + \tau_a + \tau_d = \tau_c \quad (4) $$

where $q = [q_1, q_2, q_3, q_4]$ is the arm joint angle vector, $M(q)$ is the interial matrix, $C(q, \dot{q})$ denotes Coriolis and Centrifugal term, $G(q)$ is the gravity term, τ_a denotes the vector of assistive torque, τ_d denotes the vector of disturbance torque, τ_c denotes the vector of control torque.

The needed torques are provided by cables, the first four cables provide shoulder joint with torques, and the elbow torque is generated by last two cables, the static equilibrium equations between the cable tension f and the vector of control torque τ_c are as follows:

For shoulder module:

$$ \boldsymbol{J_s^T} \begin{bmatrix} f_1 \\ \vdots \\ f_4 \end{bmatrix} + \boldsymbol{\tau_s} = 0 \quad (5) $$

For elbow module:

$$\boldsymbol{J_e^T}\begin{bmatrix} f_5 \\ f_6 \end{bmatrix} + \boldsymbol{\tau_e} = 0 \tag{6}$$

where $\boldsymbol{J^T} = \begin{bmatrix} u_1 & \cdots & u_m \\ r_1 \times u_1 & \cdots & r_m \end{bmatrix}$ represent the transformation between the cable tension and joint torque, which can be calculated through the kinematic equation. $f_i(i = 1, \cdots, 6)$ represent the tension value of each cable. τ_s and τ_e are the total required shoulder and elbow joints torques, and $\tau_c = [\tau_s, \tau_e]$.

III. CONTROL SCHEME

The cable-driven parallel mechanism with n degree of freedom is driven by $n+1$ ropes, it is necessary to study the distribution of tension among these cables. (5) and (6) give the correlation between he cable tension f_i and the joint torque τ_e, τ_s, it can be seen that the dimension of cable tension vector is larger than that of joint torque vector. Therefore, redundant solution may be obtained.

To ensure the controllability of robot movement, we should consider the controlled workspace, for cable-driven robots, controlled workspace means the platform of robot can equalize the external specific torque and force while the ropes have positive tension value.

Cable-driven exoskeleton robot include two joint with ruduence actuation, shoulder joint module and elbow joint module both has one redundant cable, thus, we can reassignment cable tension $f_i(i = 1, 2, \cdots, 6)$ with optimization. Many optimal principles can be utilized such as energy consumption minimization, smooth change in tension joint force minimization, we can parameterize these principles and set target function, to achieve characteristic tension programming algorithm. Herein, quadratic programming is chosen to calculate these cable tensions, This minimization of the quadratic sum of tension values is selected as the optimization objective of quadratic programming, this quadratic programming with nonlinear inequality constraints is expressed as:

For four ropes driven shoulder module, according to the static equilibrium equations:

$$\begin{aligned} &min. \quad g(f) = \boldsymbol{f_s^T} \cdot \boldsymbol{f_s} = \sum_{i=1}^{4} f_i^2 \\ &s.t. \quad \boldsymbol{J_s} \cdot \boldsymbol{f_s} + \boldsymbol{\tau_s} = 0 \quad and \quad f_{min} \leqslant f_i \leqslant f_{max} \end{aligned} \tag{7}$$

For two ropes driven elbow module, according to the static equilibrium equations:

$$\begin{aligned} &min. \quad g(f) = \boldsymbol{f_e^T} \cdot \boldsymbol{f_e} = \sum_{i=5}^{6} f_i^2 \\ &s.t. \quad \boldsymbol{J_e} \cdot \boldsymbol{f_e} + \boldsymbol{\tau_e} = 0 \quad and \quad f_{min} \leqslant f_i \leqslant f_{max} \end{aligned} \tag{8}$$

Due to the decoupling propety of the proposed exoskeleton, $f_i(i = 1, 2, 3, 4)$ and $f_i(5, 6)$ in Eq.(7) and Eq.(8) can be optimized separately. And the cable tension should be limited according to the practical application. In this case, f_{min} represents the minimum preload on the cable which is set as 2N, and f_{max} denotes the maximum tension allowed by the cable, considering the safety and maximum tension a rope can bear, which is set as 60N. J_s and J_e represent the matrix from cable tension to shoulder and elbow joint torque respectively.

The exoskeleton robot is a nonlinear, coupled, and redundant system. According to the theory for decoupled control of nonlinear systems, using nonlinear feedback compensation we can derive a linear decoupled control system, and the pose of robot must be measured in real time during the control process. Measuring the pose in a three dimensional space precisely and fast is relativly diffcult and costly. Moreover, it is not a desirable to obtain the pose using direct kinematics, because there would be more calculation during the run time. In this paper, an PD feedback controller combined with inverse dynamic feedforward was applied. The control scheme is shown in Fig.4. And the control law is as follows:

$$u = K_p(l_d - l) + K_d(\dot{l_d} - \dot{l}) + f_d \tag{9}$$

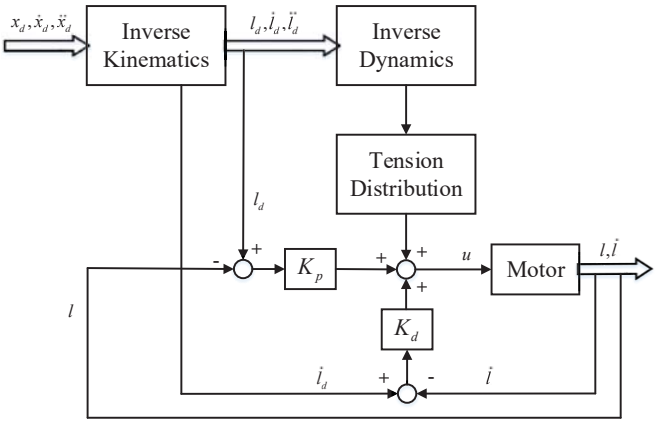

Fig. 4. Control scheme for the 4-DOF exoskeleton robot.

where $u = [u_1, u_2, \ldots, u_6]$ denotes the vector of motor torque, K_p and K_d denote feedback gain matrices. $l$and$\dot{l}$ are the feedback of cable length and cable velocity, l_d and $\dot{l}_d$ represent the desired cable length and cable velocity. They can be easily obtained through computing the inverse kinetamics, if the desired trajectory is planned offline, it is not necessary to compute optimal tension distribution at run time in feedforward control, while in the case that the trajectory is planned online, f_d is needed, which represent the tension vector calculated by the given pose.

IV. EXPERIMENTAL EVALUATION

A. Experimental System

Fig.5 show the overall experimental platform, it mainly consists of a prototype of 4-DOF exoskeleton, which connected to a humanoid robotic arm for laboratory testing. By using the robotic arm, we can measure and record motion of each joint and tension of each cables during the movement of human-robot, thus let us assess the performance of the

exoskeleton robot. Six motors are selected to drive six cables independently. To measure the tension value of the six cables, each cable was attached a load sensor, in order to measure the motion of upper limb robot, two IMU(Inertial Measurement Units) were placed on the upper arm cuff and forearm cuff respectively. Besides, six enconders were attached with six motor, to measure the velocity and position of every motor.

Using IPC(Industrial Personal Computer) as the core controller, two acquisition card were applied to collect the data of cable tension and encoder, transmit the digtal data to IPC through PCI bus. IPC is employed to operate the control algorithm, send control data to motor controller, and display the status of exoskeleton robot, the interface can also be used for monitoring the system.

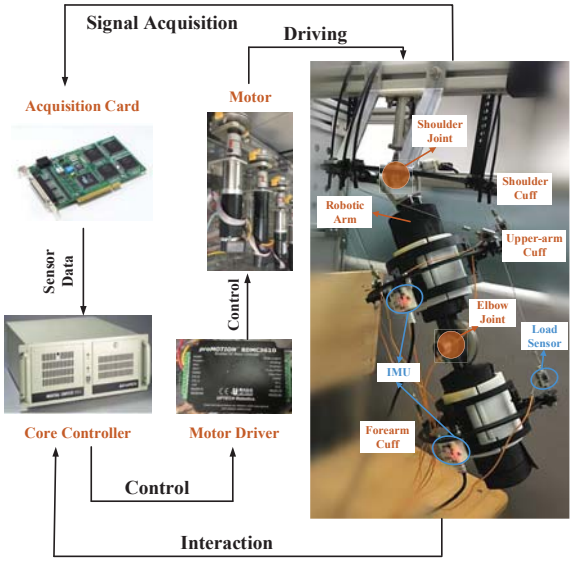

Fig. 5. A view of the overall 4-DOF exoskeleton system.

B. Experiment Result

In the experiment, the exoskeleton robot was tested in every four degree of freedom respectively, including shoulder flexion/extension motion, shoulder adduction/abduction, shoulder lateral/medial motion, and elbow flexion/extension motion. During theexperiment, the tension value and joint angles are meausred by load sensors and IMU respectively.

In order to form the desired trajectory in joint space, first we need use inverse kinematic to convert path points to joint angles, then fit each joint to a smooth function. The description of motion trajectory can be expressed by a smooth interpolation function $\theta(t)$, which is used to describe the joint angle pass the starting point and the terminating point. Cubic polynomial interpolation is selected as trajectory planning in joint space:

$$\theta(t) = a_0 + a_1 t + a_2 t^2 + a_3 t^3 \tag{10}$$

θ_0 represent the initial angle, at the terminational time t_f, joint angle is θ_f, relevant coefficients can be determined by velocity constraints and angle constraints at starting and ending points.

$$\begin{cases} a_0 = 0 \\ a_1 = 0 \\ a_2 = \dfrac{3}{t_f^2}(\theta_f - \theta_0) \\ a_3 = -\dfrac{2}{t_f^3}(\theta_f - \theta_0) \end{cases} \tag{11}$$

In the experiment, the exoskeleton drove robotic arm repetitively track the cubic polynomial trajectory, which consist of four segments. For the first part q_1(shoulder flexion/extension), the starting point θ_0 is 0^o and the ending point θ_f is -28^o, the second part q_2(shoulder adduction/abduction), the starting point θ_0 is 0^o and the ending point θ_f is -43^o, for the third part q_3(shoulder lateral/medial motion), the starting point θ_0 is 24^o and the ending point θ_f is -23^o, for the fouth part q_4(elbow flexion/extension), the starting point θ_0 is 0^o and the ending point θ_f is -38^o.

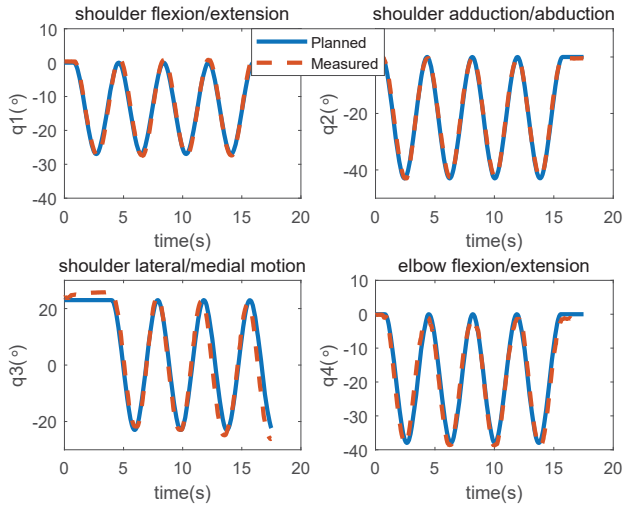

Fig. 6. Experiment result of the exoskeleton upper limb response to repetitive cubic function angle curve.

Fig.6 shows the theoretical and measured joint angle, which demonstate the tracking result using the controller mention in the previous section, we can see from the result that the measured values are close to the planned trajectory, which means that the proposed controller has a good performance in the practical application.

The tension value of each cable measured by load sensor is shown in Fig.7, using the tension distribution algorithm based on quadratic programing algorithm, we can see from the graph that the cable tensions are within the maximum tension range. Due to some non-linear factors of the sensor itself and measurement noise, the sensor data will fluctuate greatly, which has a certain impact on the control system.

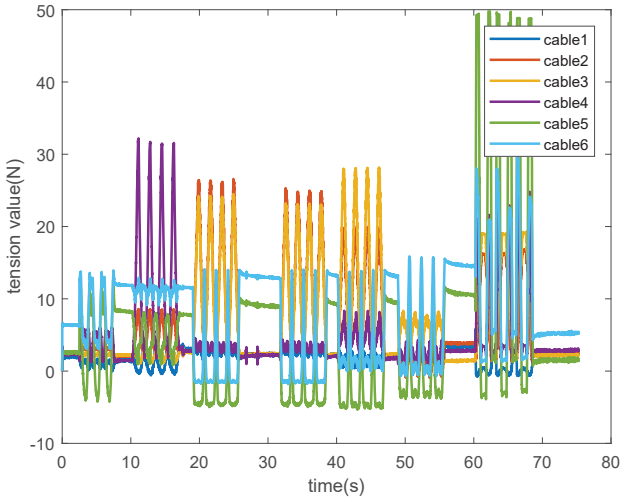

Fig. 7. Tension values in all cables.

V. CONCLUSION

In this paper, a motion controller for a 4-DOF cable-driven exoskeleton robot was proposed, which drive humanoid upper limb with set trajectory with six cables. The cable-driven design offers motion assistance for 3-DOF shoulder joint and 1-DOF elbow joint, the cable-driven exoskeleton have many advantages such as being light-weight and without the need for accurate joint alignment between the exoskeleton and human joints, which can be used as a rehabilitation training device for stoke patients. In this paper, the workspace condictions and the dynamics of the 4-DOF exoskeleton robot are described, based on the this, motion control scheme using nonlinear feedforwad control law is proposed and implemented on the protype exoskeleton robot, considering the propety of the cable and safety of robot, cable tension optimizer based on quadratic programing algorithm is developed to calculate the required cable tensions. At last, by experiment, sensor data is tested, from the experiment result, the effectiveness of the device is demonstrated.

Further studies will consider experminent on healthy human arm and petients on the promise of safety, to verify its effectiveness and improve its functionality.

ACKNOWLEDGMENT

This work is supported by National Natural Science Foundation of China Grant Nos. 51675018, 61773042 and 51475033.

REFERENCES

[1] C. D. Wolfe, "The impact of stroke," *British Medical Bulletin*, vol. 56, no. 2, pp. 275–286, 2000.

[2] N. J. Kassebaum, M. Arora, R. M. Barber *et al.*, "Global, regional, and national disability-adjusted life-years (dalys) for 315 diseases and injuries and healthy life expectancy (hale), 1990–2015: a systematic analysis for the global burden of disease study 2015," *The Lancet*, vol. 388, no. 10053, pp. 1603–1658, 2016.

[3] G. A. Donnan, M. Fisher, M. Macleod, and S. M. Davis, "Stroke," *The Lancet*, vol. 371, no. 9624, pp. 1612–1623, May 2008.

[4] L. Liu, D. Wang, K. L. Wong, and Y. Wang, "Stroke and Stroke Care in China," *Stroke*, vol. 42, no. 12, pp. 3651–3654, Dec. 2011.

[5] J. C. Perry, J. Rosen, and S. Burns, "Upper-Limb Powered Exoskeleton Design," *IEEE/ASME Transactions on Mechatronics*, vol. 12, no. 4, pp. 408–417, Aug. 2007.

[6] N. Hogan, H. Krebs, J. Charnnarong, P. Srikrishna, and A. Sharon, "MIT-MANUS: a workstation for manual therapy and training I," in *Proceedings IEEE International Workshop on Robot and Human Communication*, 1992, pp. 161–165.

[7] T. Nef, M. Guidali, and R. Riener, "ARMin III arm therapy exoskeleton with an ergonomic shoulder actuation," *Applied Bionics and Biomechanics*, vol. 6, no. 2, pp. 127–142, Jul. 2009.

[8] S. J. Ball, I. E. Brown, and S. H. Scott, "A planar 3-DOF robotic exoskeleton for rehabilitation and assessment," in *Annual International Conference of the IEEE Engineering in Medicine and Biology Society*, Aug. 2007, pp. 4024–4027.

[9] N. Hogan, H. I. Krebs, J. Charnnarong, P. Srikrishna, and A. Sharon, "Mit-manus: a workstation for manual therapy and training II," *Proceedings of SPIE - The International Society for Optical Engineering*, pp. 161–165, 1993.

[10] L. E. Kahn, W. Z. Rymer, and D. J. Reinkensmeyer, "Adaptive assistance for guided force training in chronic stroke," in *The 26th Annual International Conference of the IEEE Engineering in Medicine and Biology Society*, vol. 1, Sep. 2004, pp. 2722–2725.

[11] T. Nef, G. Quinter, R. Mller, and R. Riener, "Effects of Arm Training with the Robotic Device ARMin I in Chronic Stroke: Three Single Cases," *Neurodegenerative Diseases*, vol. 6, no. 5-6, pp. 240–251, 2009.

[12] T. Nef, M. Guidali, V. Klamroth-Marganska, and R. Riener, "Armin-exoskeleton robot for stroke rehabilitation," in *World Congress on Medical Physics and Biomedical Engineering*, Sep. 2009, pp. 127–130.

[13] R. S. Calabr, M. Russo, A. Naro, D. Milardi, T. Balletta, A. Leo, S. Filoni, and P. Bramanti, "Who May Benefit From Armeo Power Treatment? A Neurophysiological Approach to Predict Neurorehabilitation Outcomes," *PM&R*, vol. 8, no. 10, pp. 971–978, Oct. 2016.

[14] H. Kino, N. Okubo, T. Ikeda, and H. Ochi, "Error Evaluation Method of Approximated Inverse Kinematics for Parallel-Wire Driven System Basic Study for Three-Wire Planar System ," *Journal of Robotics and Mechatronics*, vol. 28, no. 6, pp. 808–818, Dec. 2016.

[15] A. Frisoli, C. Chisari, E. Sotgiu, C. Procopio, M. Fontana, B. Rossi, and M. Bergamasco, "Rehabilitation Training and Evaluation with the L-EXOS in Chronic Stroke," in *Impact Analysis of Solutions for Chronic Disease Prevention and Management*, Berlin, Heidelberg, 2012, vol. 7251, pp. 242–245.

[16] S. Balasubramanian, M. Perez, B. Shepard, E. Koeneman, and J. K. and, "Rupert: An exoskeleton robot for assisting rehabilitation of arm functions," in *2008 Virtual Rehabilitation*, Aug 2008, pp. 163–167.

[17] S.-R. Oh and S. K. Agrawal, "The feasible workspace analysis of a set point control for a cable-suspended robot with input constraints and disturbances," *IEEE Transactions on Control Systems Technology*, vol. 14, no. 4, pp. 735–742, 2006.

[18] X. Cui, W. Chen, X. Jin, and S. K. Agrawal, "Design of a 7-DOF Cable-Driven Arm Exoskeleton (CAREX-7) and a Controller for Dexterous Motion Training or Assistance," *IEEE/ASME Transactions on Mechatronics*, vol. 22, no. 1, pp. 161–172, Feb. 2017.

[19] S. Roderick, M. Liszka, C. Carignan, S. Roderick, M. Liszka, and C. Carignan, "Design of an arm exoskeleton with scapula motion for shoulder rehabilitation," in *2005 International Conference on Advanced Robotics, ICAR '05, Proceedings*, July 2005, pp. 524–531.

[20] S. K. Mustafa and S. K. Agrawal, "On the Force-Closure Analysis of n-DOF Cable-Driven Open Chains Based on Reciprocal Screw Theory," *IEEE Transactions on Robotics*, vol. 28, no. 1, pp. 22–31, Feb. 2012.

[21] X. Cui, W. Chen, G. Yang, and Y. Jin, "Closed-loop control for a cable-driven parallel manipulator with joint angle feedback," in *2013 IEEE/ASME International Conference on Advanced Intelligent Mechatronics*, July 2013, pp. 625–630.

[22] W. Chen, X. Cui, G. Yang, J. Chen, and Y. Jin, "Self-feedback motion control for cable-driven parallel manipulators," *Proceedings of the Institution of Mechanical Engineers, Part C: Journal of Mechanical Engineering Science*, vol. 228, no. 1, pp. 77–89, 2014.